



Identification of the plastic zone using digital image correlation

M. Rossi, M. Sasso, G. Chiappini, E. Mancini, D. Amodio

Polytechnic University of Marche

m.rossi@univpm.it, m.sasso@univpm.it, g.chiappini@univpm.it, e.mancini@univpm.it, d.amodio@univpm.it

ABSTRACT. In this paper Digital Image Correlation (DIC) is used to study the evolution of the plastic zone close to a crack tip. A modified CT-specimen was used in order to fulfill the plane stress condition. The strain field around the crack tip was measured using two cameras and stereo DIC, so that out-of-plane movements are taken into account. Then, the Virtual Fields Method was used to identify the plastic zone, looking at the parts of the specimen which deviates from the linear elastic behavior. With such approach, it was possible to individuate the onset of plasticity close to the crack tip and follow its evolution. A comparison with FEM results is also provided.

KEYWORDS. Digital image correlation; Plastic zone; Virtual Fields Method; Fracture mechanics.

INTRODUCTION

The Virtual Fields Method (VFM) is a technique that can be used to identify the mechanical properties of materials, starting from full field measurements [1]. During the years, such a technique was extended to many fields of mechanical engineering [2-5].

The VFM exploits the principle of virtual work to identify the material properties using experimental tests which produce heterogeneous strain fields. In the field of plasticity, the VFM is gaining increasing interest [6, 7] because large amount of information can be obtained from a single test, moreover the minimization procedure is usually faster than FE updating methods.

In this paper, the VFM is used to identify the plastic zone on a crack tip. The transition between plastic and elastic behaviour can be easily obtained by FE computations but it is not possible to directly individuate it from experimental measurements of the strain field. The identification is performed starting from the strain field measured close to the crack tip. Although this area is rather small, ($1 \sim 4 \text{ mm}^2$) the high resolution of recent digital cameras and the improvements in the full-field measurement techniques (e.g. DIC, grid method) allow nowadays to very accurate strain measurements with a high grade of spatial resolution and noise reduction even on small surfaces [9, 10].

Afterwards, in order to apply the VFM, suitable virtual fields are defined so that the contribution of the external forces is zeroed. These virtual fields are generated using piecewise functions [11], the virtual displacement on the nodes placed at the boundary of the inspected area are set to zero. An error function is then developed to assess the zones where the elastic behavior is not fulfilled. This error indicates the deviation from the linear elastic behavior, when it exceeds a threshold value, the corresponding material point is considered part of the plastic zone. It is worth noting that no force measurement is required with this approach.

The procedure was validated by means of simulated experiments using a FE model [12]. In this paper the first experimental results are shown. A test was conducted on a modified CT specimen and the evolution of the plastic zone is evaluated.



THEORETICAL BACKGROUND

The plastic zone is obtained applying the VFM. The VFM relies on the principle of virtual works that, for a solid of any shape of volume V and surface ∂V , if there are no body forces acting on the solid, can be written as

$$\int_V \boldsymbol{\sigma} : \boldsymbol{\varepsilon}^* dV = \int_{\partial V} \mathbf{T} \cdot \mathbf{u}^* dS \tag{1}$$

where $\boldsymbol{\sigma}$ is the stress tensor, \mathbf{T} is a surface force acting at the boundary and \mathbf{u}^* and $\boldsymbol{\varepsilon}^*$ are a kinematically admissible virtual fields and the corresponding virtual strain fields, respectively. In case of in-plane tests with constant thickness, the problem reduces to a 2-D situation and Eq. 3 can be rewritten as:

$$t \int_S \boldsymbol{\sigma} : \boldsymbol{\varepsilon}^* dS = t \int_{\partial S} \mathbf{T} \cdot \mathbf{u}^* dl \tag{2}$$

where t is the specimen thickness. Considering an isotropic elastic material behaviour, the stress tensor can be written as a function of strain field according to the constitutive equations, for plane stress it follows:

$$\begin{pmatrix} \sigma_{xx} \\ \sigma_{yy} \\ \tau_{xy} \end{pmatrix} = \frac{E}{1-\nu^2} \begin{bmatrix} 1 & \nu & 0 \\ \nu & 1 & 0 \\ 0 & 0 & \frac{1-\nu}{2} \end{bmatrix} \begin{pmatrix} \varepsilon_{xx} \\ \varepsilon_{yy} \\ \gamma_{xy} \end{pmatrix} \tag{3}$$

with E and ν which are the Young's modulus and the Poisson's ratio, respectively. The strain field is the one measured during the experiment by a full-field optical technique. The virtual fields involved in Eq. 4 can be arbitrarily chosen if they are kinematically admissible [1]. They can be defined using piecewise functions as it occurs in FE models [1,11]. In this case the virtual displacement \mathbf{u}^* is written as a function of the nodal coordinates $u(e)$ of an element according to the element shape functions \mathbf{N} :

$$\mathbf{u}^* = \mathbf{N} \mathbf{u}^{(e)} \tag{4}$$

The strain can be obtained as well from the nodal coordinates as:

$$\boldsymbol{\varepsilon}^* = \mathbf{B} \mathbf{u}^{(e)} \tag{5}$$

In the present case a regular square grid of four elements was used, the 8 nodes at the boundary are kept fixed while the internal node is moved. In such a way the virtual displacement at the boundary is equal to zero and the second term of Eq. 4 vanishes. 24 independent virtual fields were generated by varying the displacement U^* of the central node as follows:

$$\mathbf{U}^* = \{ \cos \mathcal{G}, \sin \theta \} \quad \text{with} \quad \mathcal{G} = [0 : \pi / 12 : 2\pi[\tag{6}$$

When the material has a linear elastic behaviour, the equilibrium is respected and the first term of Eq.4 is identically null in each zone of the specimen. Close to the crack tip, however, the material behaviour deviates from elasticity because plastic deformation locally occurs. In this case, Eq. 4 is not valid anymore, this discrepancy can be considered as an indication of the plasticity occurrence. With this assumption, an error function Err is defined as:

$$Err = \frac{1}{\bar{\varepsilon}} \frac{1}{N_v} \sum_i \frac{1}{S} \left| \int_S \boldsymbol{\sigma} : \boldsymbol{\varepsilon}_i^* dS \right| \tag{7}$$

where N_v is the number of independent virtual fields employed, i.e. 24 in this case. The unit of this error is a specific energy. The larger the error function the most likely the inspected zone undergoes plastic deformation. The error is normalized on the surface area S so that its value is not influenced by its size. Indeed, the area can be varied in order to include more or less measurement points. The error functions is also influenced by the amount of strain in the investigated zone. In order to have a fair comparison between zones with different levels of strain, the normalization parameter $\bar{\varepsilon}$ is also introduced defined as:

$$\bar{\varepsilon} = \frac{1}{S} \left| \int_S \varepsilon_{VM} dS \right| \quad (8)$$

where ε_{VM} is the equivalent von Mises strain. It is worth underlying that no other assumptions are made on the plasticity law, therefore the identification of the plasticity material properties are not necessary to detect the plastic zone. The area of the virtual field is moved along the measured strain field as a sort of “probe” which detects the likelihood of plastic deformation occurrence inside the area. In such a way, it is possible to define an error map close to the crack tip.

EXPERIMENTS

A modified CT-specimen was used in the experimental test. Fig. 1 illustrates an example of CT-specimen according to the ASTM [13]. The dimension of the specimens depends on the parameter W , which allows to scale the specimen according to the thickness. In this case, since Eq. 5 is only valid for plane stress, the CT-specimen was modified so that the thickness was small compared to the in-plane dimensions. The specimen was cut from a 3mm thick sheet metal of AISI 304 steel. A value of $W=100\text{mm}$ is used for all the other dimensions.

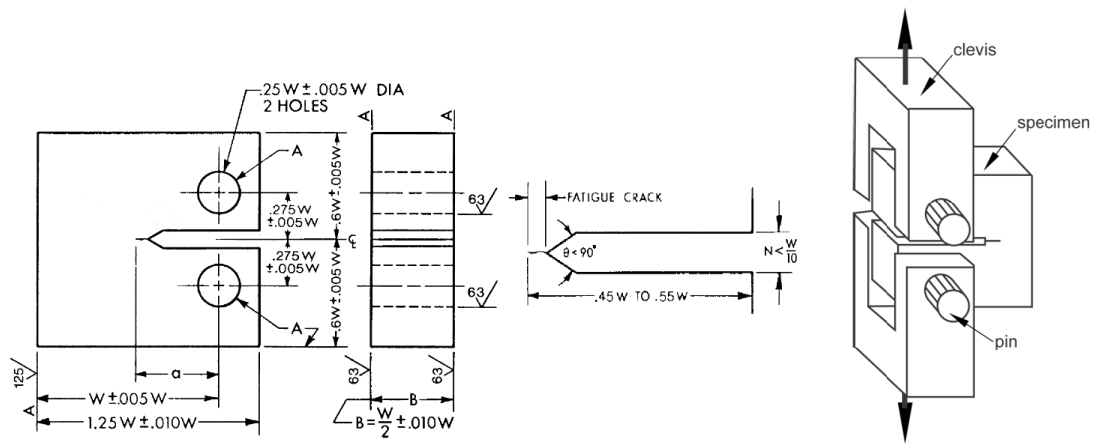


Figure 1: Scheme of the used CT-specimen.

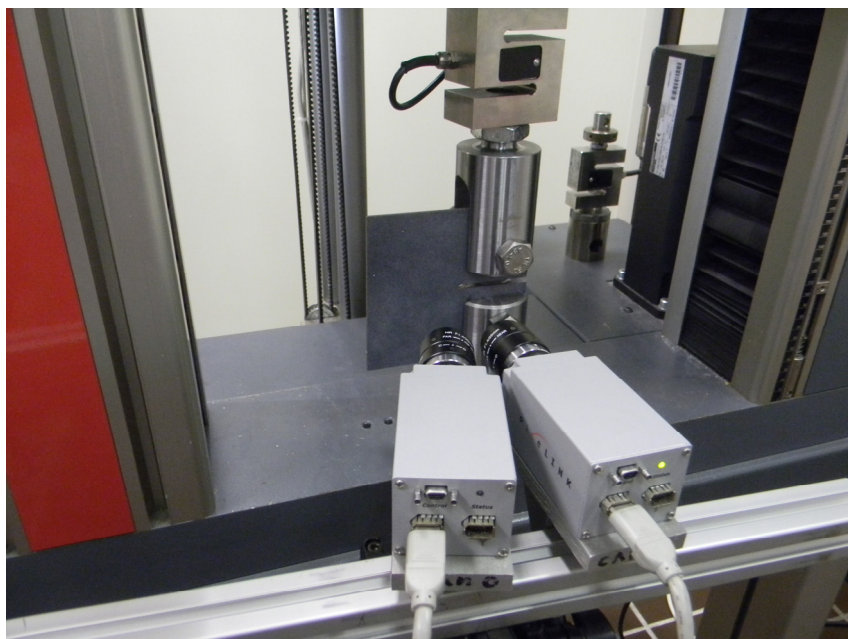


Figure 2: Experimental set-up.



In Fig. 2 the experimental set-up is shown, the modified CT-specimen was loaded using suitable fixture which guarantees an in-plane loading. Buckling occurs at large deformation, however it was possible to apply up to 5 kN to the specimen before a consistent out of plane movement was measured.

The strain field measurement was obtained by means of stereo DIC. Two cameras have been used with an angle of around 15° . A speckle pattern was sprayed onto the specimen surface. The investigated area is around 6×6 mm close to the crack tip. A global DIC approach is used using a regular mesh of 32×32 pixels that corresponds to 0.8×0.8 mm in actual units. The strain at each pixel was then obtained using the shape function of the elements

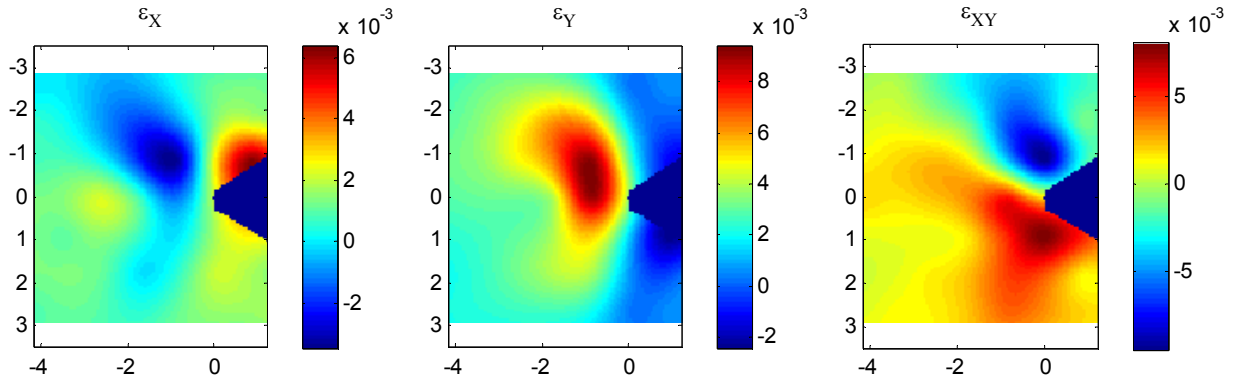


Figure 3: Measured strain field.

RESULTS AND DISCUSSIONS

The error function obtained from Eq. 7 is plotted for different values of the tensile force, see Fig. 4. The same contour limits are used for all graphs. As the force increases, the error function also increases close to the crack tip showing the evolution of the plastic zone. A certain amount of noise is present, but the evolution of the plastic zone is clearly visible.

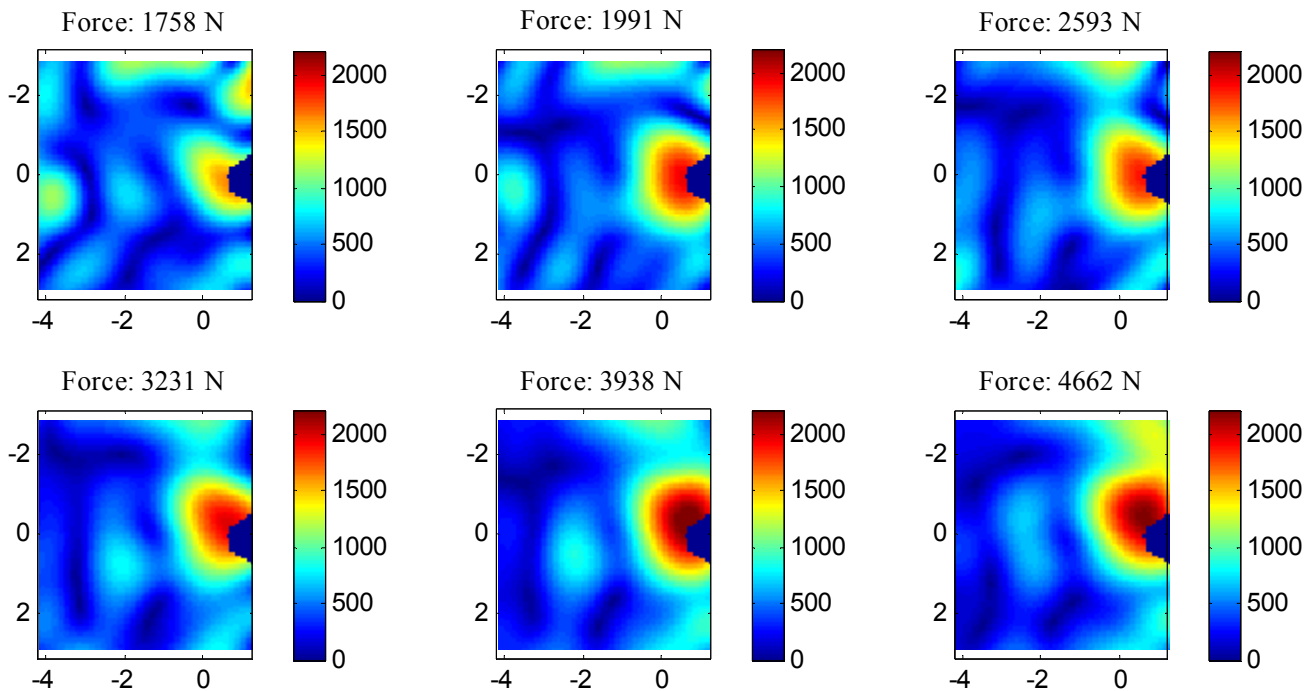


Figure 4: Identification of the plastic radius.



In Fig. 5, the plastic zone computed by FEM for two levels of force, namely the first and the last of Fig. 4, are illustrated. Qualitatively, a reasonably good match is obtained with the experimental results. The FEM model was built using the actual mechanical properties of the material obtained by means of uniaxial tensile tests.

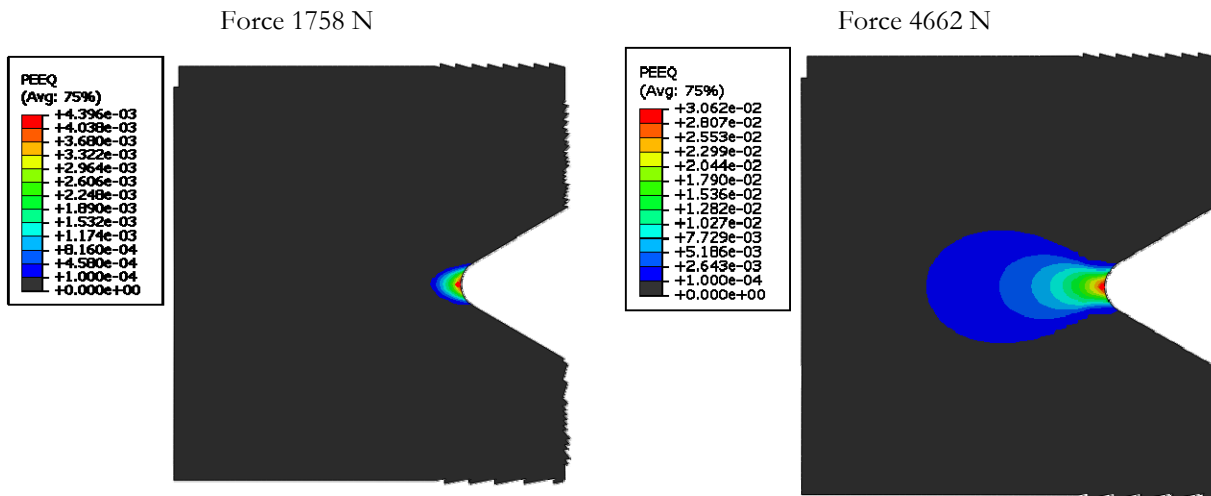


Figure 5: Plastic zone evaluated by FEM for the same specimen and same load levels

CONCLUSIONS

A procedure to evaluate the plastic zone close to the crack tip starting from full field DIC measurement data is presented. A modified CT specimen was used to ensure the plane stress condition in the area of interest. Test were conducted at different load levels, stereo DIC was used to extract the strain field close to the crack tip, then the VFM was used to look at the zones which deviate from the linear elastic behavior. Qualitatively, a good match is found between the error maps and the plastic zone evaluated by FEM. In future works more effort will be put on quantitatively evaluating the plastic zone setting a suitable threshold to the level of error measured.

REFERENCES

- [1] Pierron, F., Grédiac, M., *The Virtual Fields Method*, Springer, (2012).
- [2] Palmieri, G., Sasso, M., Chiappini, G., Amodio, D., *Virtual Fields Method on Planar Tension Tests for Hyperelastic Materials Characterisation*, *Strain*, 47 (2011) 196-209.
- [3] Guélon, T., Toussaint, E., Le Cam, J.-B., Promma, N., Grédiac, M., *A new characterisation method for rubber*, *Polymer Testing*, 28 (2009) 715-723.
- [4] Pierron, F., Forquin, P., *Ultra-High-Speed Full-Field Deformation Measurements on Concrete Spalling Specimens and Stiffness Identification with the Virtual Fields Method*, *Strain*, 48 (2012) 388-405.
- [5] Giraudeau, A., Pierron, F., *Identification of stiffness and damping properties of thin isotropic vibrating plates using the virtual fields method. Theory and simulations*, *J. Sound. Vib.* 284 (2005) 757-781.
- [6] Rossi, M., Pierron, F., *Identification of plastic constitutive parameters at large deformations from three dimensional displacement fields*, *Comput. Mech.*, 49 (2012) 53-71.
- [7] Grédiac, M., Pierron, F., *Applying the virtual fields method to the identification of elasto-plastic constitutive parameters*, *Int. J. Plasticity*, 22 (2006) 602-627.
- [8] Avril, S., Bonnet, M., Bretelle, A. S., Grédiac, M., Hild, F., Ienny, P., Latourte, F., Lemosse, D., Pagano, S., Pagnacco, E., Pierron, F., *Overview of identification methods of mechanical parameters based on full-field measurements*, *Exp. Mech.*, 48 (2008) 381-402.
- [9] Bornert, M., Brémand, F., Doumalin, P., Dupré, J.-C., Fazzini, M., Grédiac, M., Hild, F., Mistou, S., Molimard, J., Orteu, J.-J., Robert, L., Surrel, Y., Vacher, P., Wattrisse, B., *Assessment of digital image correlation measurement errors: methodology and results*, *Exp. Mech.*, 49 (2009) 353-370.



- [10] Moulart, R., Rotinat, R., Pierron, F., Lerondel, G., On the realization of microscopic grids for local strain measurement by direct interferometric photolithography, *Opt. Laser. Eng.*, 45 (2007) 1131–1147.
- [11] Avril, S., Grédiac, M., Pierron, F., Sensitivity of the virtual fields method to noisy data, *Comput. Mech.*, 34 (2004) 439–452.
- [12] Rossi, M. Fardmoshiri, M., Sasso, M., Amodio, D., Application of the Virtual Fields Method to fracture mechanics, In: *Convegno Nazionale IGF XXII, Roma, Italia, (2013) 322-331*
- [13] ASTM Standards, Standard Test Method for Plane-Strain Fracture Toughness of Metallic Materials, ASTM E399- 90, American Society for Testing and Materials, Philadelphia, (1997).